



# Integrating Second Order Sliding Mode Control and Anomaly Detection Using Auto-Encoder for Enhanced Safety and Reliability of Quadrotor UAVs

Saman Yazdannik<sup>1</sup>, Shamimeh Saniesales<sup>2\*</sup>, Morteza Tayefi<sup>1</sup>, Reza Esmaelzadeh<sup>2</sup>, Mostafa Khazaei<sup>2</sup>

1. Faculty of Aerospace, K. N. Toosi University of Technology, Iran

2. Faculty of Aerospace, Malek Ashtar University of Technology, Iran

\* [shamim.saniesales7@gmail.com](mailto:shamim.saniesales7@gmail.com)

## Abstract

This paper presents a comprehensive framework for enhancing the safety and reliability of quadrotor UAVs by integrating second-order sliding mode control (2-SMC) and an advanced anomaly detection and prediction system based on machine learning and AI. The paper addresses the challenges of designing controllers for quadrotors by proposing a novel sliding manifold approach divided into two subsystems for accurate position and attitude tracking. The paper also provides a detailed analysis of the nonlinear coefficients of the sliding manifold using Hurwitz stability analysis. It demonstrates the effectiveness of the proposed method through extensive simulation results. To further assess the safety and reliability of the quadrotor, an anomaly detection and prediction system is integrated with the position and attitude tracking control. The system utilizes machine learning and AI techniques to identify and predict abnormal behaviours or faults in real time, enabling the quadrotor to quickly and effectively respond to critical situations. The proposed framework provides a promising approach for designing robust and safe controllers for quadrotor UAVs. It demonstrates the potential of advanced machine learning and AI techniques for enhancing the safety and reliability of autonomous systems.

**Keywords:** Anomaly detection; Auto-encoder; Fault detection; Machine learning; Quadrotor UAVs; Safety; second-order sliding mode control (2-SMC).

## 1. Introduction

The research community, including industry, government, and academia, has recently demonstrated a growing interest in Unmanned Aerial Vehicles (UAVs) [1-4]. The appeal of UAVs can be attributed to their ability to perform various applications such as search and rescue missions, law enforcement, mapping, aerial cinematography, power plant inspection, and wildfire surveillance [5]. The potential to eliminate human pilots from danger and the size and cost of unmanned aircraft is undeniably attractive; however, their mission capabilities, efficiency, and flexibility must be compared to those of traditional manned aircraft. However, developing intelligent and

data-driven controllers for UAVs necessitates working with the real system to learn their nonlinear and complex dynamics. A recent study proposed a novel approach to mitigate the risks associated with costly failures during flight tests [6]. The authors have introduced a vehicle-in-the-loop (VIL) platform that integrates the real system into a simulation loop, providing a safe and effective solution for controller design. By hinging the multirotor UAV to a shaft that allows angular motion while restricting translational motion, the platform enables the learning of the drones' dynamics without the need for risky flight tests. The study demonstrates the effectiveness of the VIL platform by implementing a proportional-integral-derivative (PID) and a brain emotional learning-based

intelligent controller (BELBIC) for tracking various flight trajectories, showing superior performance of BELBIC in the test.

The quadrotor UAV is a Vertical Take-Off and Landing (VTOL) aircraft that utilizes four rotors to achieve a range of benefits such as increased payload capacity, inherent hover stability, and enhanced manoeuvrability. Compared to conventional aircraft, the quadrotor UAV boasts reduced mechanical complexity, making it an attractive option for various applications. Its range of movements includes precession motion, which is eliminated by designing the front and rear rotors to rotate opposite to the left and right propellers. This design removes reactive torque around the vertical coordinate axis. The quadrotor UAV can also perform hover motion by maintaining the same rotational velocity of each propeller. Roll and pitch motion can be achieved by varying the rotational velocity difference between the opposing rotors, causing the vehicle to tilt towards the slowest propeller. Yaw motion is produced by adjusting the rotational velocity of neighbouring rotors differently from the others, resulting in the vehicle tilting towards the two slower propellers. Vertical motion is acquired by adjusting the rotational velocity of all rotors by the same amount. In contrast, horizontal motion is achieved by initially rolling or pitching the vehicle to change the direction of the thrust vector and then generating a forward component [1].

Furthermore, in the field of unmanned aerial vehicles (UAVs), there has been significant research on vibration control and attitude stabilization of flexible spacecraft. Recently, a paper by [7] proposed a PID-based sliding mode fault-tolerant scheme to preserve the system against external disturbances, rigid-flexible body interactions, and partial actuator failures. The authors combined the advantages of PID and sliding mode control to enhance the robustness, reduce steady-state errors, and minimize the computational burden. Their study demonstrated the effectiveness of the sliding mode controller in accommodating various actuator fault scenarios and maintaining healthy behaviour. Additionally, an active vibration control (AVC) law utilizing a strain rate feedback (SRF) algorithm and piezoelectric (PZT) sensors/actuators was implemented to compensate for residual vibrations caused by attitude dynamics and actuator failures. Numerical simulations showcased the superiority of the proposed schemes in fault tolerance and robustness compared to conventional approaches.

This paper focuses on a small quadrotor UAV's position and attitude-tracking control. In real-world missions, the stability of the aircraft can be easily disrupted by sudden changes in commands. Thus, developing a flight controller capable of providing precise and reliable control to the aircraft is crucial for the success of the flight process. For that purpose, we add an

anomaly detection and prediction system on a small quadrotor UAV's position and attitude tracking control. Adding an anomaly detection system to a small quadrotor UAV's position and attitude tracking control can significantly enhance its safety and reliability. Anomaly detection is a process of identifying unexpected events or deviations from normal behaviour. By implementing an anomaly detection system, the quadrotor UAV can quickly detect anomalies caused by sensor failures, environmental changes, or unexpected disturbances and take appropriate action to prevent accidents. The process of implementing an anomaly detection system involves defining normal behaviour, choosing a detection method, implementing the system, testing it, and monitoring and maintaining it over time. Following these steps, the quadrotor UAV can operate safely and effectively in various conditions [8].

Several extended sliding mode control (SMC) methods have been proposed to design flight controllers for quadrotor aircraft [9-13]. In [9], a robust second-order sliding mode controller was proposed to stabilize the attitude of a quadrotor helicopter, overcoming the chattering phenomenon in classical (first-order) sliding mode control while preserving the invariance property of sliding mode. In [10], an SMC approach was proposed to stabilize a class of cascaded underactuated systems, with the quadrotor helicopter's dynamical model serving as an example to illustrate the proposed SMC. The use of SMC strategies in these works was necessary to compensate for external disturbances, with the wind as a specific disturbance taken into account to demonstrate the control algorithm's robustness in the quadrotor's flight process [9,15]. A second-order sliding mode control (2-SMC) was proposed to improve the performance of control systems for second-order uncertain plants using an equivalent approach [16]. In [17], an adaptive second-order sliding mode (SOSM) controller with a nonlinear sliding surface was proposed. However, in the most existing literature on quadrotor UAV control, the coefficients of the defined sliding manifolds are taken as special values and given directly in simulations. To further explore information about the coefficients' characteristics, the condition of Hurwitz's stability can be used to calculate the coefficients of sliding manifolds.

The dynamics model is decomposed into two subsystems to achieve good tracking control performance of a quadrotor aircraft using 2-SMC. The fully actuated subsystem can converge to its linear switching surfaces, but the underactuated subsystem requires the stabilization of a nonlinear sliding manifold or internal dynamics. Previous work proposed a linear sliding manifold for an underactuated system [18,19], combining position and velocity tracking errors to obtain four coefficients. Using Lyapunov theory, the 2-SMC law guarantees the stability of the subsystem, but the sliding motion is complex and nonlinear. To simplify the design of the switching

surface, the nonlinear sliding manifold is linearized around desired equilibrium points, and coefficients are calculated using Hurwitz stability. This results in an equivalent linearized switching manifold that can be controlled through full-state linear feedback.

This paper proposes a method based on the second-order sliding mode control (2-SMC) to design controllers for a small quadrotor UAV. Our approach builds on the work presented in the original paper on 2-SMC control of quadcopters by En-Hui Zheng et al. [20], which proposed a sliding manifold design for position and attitude tracking control. To enhance the performance of the quadrotor system, we extend the sliding manifold approach by incorporating a fault detection system using a machine learning method. Specifically, we divide the dynamical model of the quadrotor into two subsystems, a fully actuated subsystem and an underactuated subsystem, and construct sliding manifolds for each subsystem with varying coefficients. To obtain the nonlinear coefficients of the sliding manifold, we use Hurwitz stability analysis during the solving process. Flight controllers are derived using Lyapunov theory to ensure all system state trajectories reach and remain on the sliding surfaces. Our proposed control method is validated through extensive simulation results, demonstrating its effectiveness in achieving position and attitude-tracking control with added fault detection capabilities. The original paper on 2-SMC control of quadcopters is also cited in this paper as a foundation for our work.

The paper is organized as follows. It begins by presenting the dynamical model of the quadrotor. Then, the problem is formulated. Next, the quadrotor flight controller design based on 2-SMC is detailed. A machine learning approach for an anomaly detection and prediction system is added to a small quadrotor UAV's position and attitude tracking control. Finally, the paper concludes with a summary of the findings.

## 2. Quadrotor dynamical model

Figure 1 provides a detailed illustration of the quadrotor aircraft. The dynamical model of the quadrotor is formulated with respect to the body-frame  $B(Oxyz)$  and the earth-frame  $e(Oxyz)$ . The position of the center of gravity of the quadrotor in the earth frame is represented by a vector  $[x, y, z]'$ , while its linear velocity in the earth frame is represented by a vector  $[u, v, w]'$ . The angular velocity in the body frame is represented by a vector  $[p, q, r]'$ , and the total mass of the aircraft is denoted by  $m_s$ . The acceleration of gravity is denoted by  $g$ , and  $l$  represents the distance from the centre of each rotor to the centre of gravity.

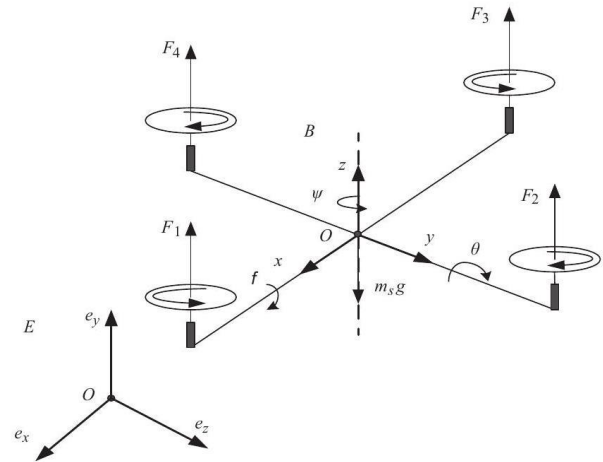


Figure 1. Quadrotor Dynamics

The quadrotor's orientation is described by the rotation matrix:  $e \rightarrow B$ , which is dependent on the three Euler angles  $[\phi, \theta, \psi]'$  that corresponds to the roll, pitch, and yaw angles, respectively. These angles have bounds of  $(-\pi/2 < \phi < \pi/2)$  for the roll angle,  $(-\pi/2 < \theta < \pi/2)$  for the pitch angle, and  $(-\pi < \psi < \pi)$  for the yaw angle. Compensation for the rotation of the quadrotor's body is necessary to achieve accurate position control. This compensation is achieved by using the transpose of the rotation matrix:

$$R = R(\phi, \theta, \psi) = R(z, \psi)R(y, \theta)R(x, \phi)$$

$$R(z, \psi) = \begin{bmatrix} \cos \psi & -\sin \psi & 0 \\ \sin \psi & \cos \psi & 0 \\ 0 & 0 & 1 \end{bmatrix},$$

$$R(y, \theta) = \begin{bmatrix} \cos \theta & 0 & \sin \theta \\ 0 & 1 & 0 \\ -\sin \theta & 0 & \cos \theta \end{bmatrix},$$

$$R(x, \phi) = \begin{bmatrix} 1 & 0 & 0 \\ 0 & \cos \phi & -\sin \phi \\ 0 & \sin \phi & \cos \phi \end{bmatrix}. \quad (1)$$

The rotational and translational kinematic equations are derived using the rotation matrix. The translational kinematics equation is expressed as:

$$\dot{v}_e = R \cdot v_B \quad (2)$$

where  $v_e = [u_0, v_0, w_0]'$  and  $v_B = [u_b, v_b, w_b]'$  represent the linear velocities of the centre of mass in the earth frame and body frame, respectively.

The rotational kinematics relationship can be derived from the derivative of the rotation matrix and a skew-symmetric matrix [18].

$$\dot{\Phi} = H^{-1}\Omega$$

$$\begin{bmatrix} \dot{\phi} \\ \dot{\theta} \\ \dot{\psi} \end{bmatrix} = \begin{bmatrix} 1 & \sin \phi \tan \theta & \cos \phi \tan \theta \\ 0 & \cos \phi & -\sin \phi \\ 0 & \sin \phi \sec \theta & \cos \phi \sec \theta \end{bmatrix} \begin{bmatrix} p \\ q \\ r \end{bmatrix} \quad (3)$$

The angular velocities in the body-frame, denoted by  $\Omega = [p, q, r]'$ , and the three Euler angles representing roll, pitch, and yaw, denoted by  $\Phi = [\phi, \theta, \psi]'$ , are related through the given equation.

The quadrotor's translational movement is described by the following equation [22, 23]:

$$m_s \ddot{P} + m_s R_{j,3} = f \tag{4}$$

where  $P = [x, y, z]'$  denotes the position of the quadrotor's centre of gravity in the earth-frame,  $f = R_{j,3} \cdot u_1 + a$  represents the total force applied to the quadrotor in the z-axis direction,  $m$  is the mass of the aircraft,  $g$  is the acceleration due to gravity, and  $a = [K_1 \cdot \dot{x}, K_2 \cdot \dot{y}, K_3 \cdot \dot{z}]'$  is the air drag matrix, where  $K_1, K_2,$  and  $K_3$  are the drag coefficients in the  $e_x, e_y,$  and  $e_z$  directions, respectively. The term  $R_{j,3}$  represents the third column of the rotation matrix.

$$\begin{cases} \dot{x} = \frac{1}{m_s} (\cos \phi \sin \theta \cos \psi + \sin \phi \sin \psi) u_1 - \frac{K_1 \dot{x}}{m_s} \\ \dot{y} = \frac{1}{m_s} (\cos \phi \sin \theta \sin \psi - \sin \phi \cos \psi) u_1 - \frac{K_2 \dot{y}}{m_s} \\ \dot{z} = \frac{1}{m_s} (\cos \phi \cos \theta) u_1 - g - \frac{K_3 \dot{z}}{m_s} \end{cases} \tag{5}$$

Given that the quadrotor aircraft exhibits both rigidity and symmetry, its rotational kinetic equation can be formulated as follows:

$$\frac{d}{dt}(J\Omega) = M \tag{6}$$

The inertia matrix of the quadrotor is denoted by  $J = \text{diag}[I_x, I_y, I_z]$ , where  $I_x, I_y$  and  $I_z$  represent the inertia of the quadrotor. The total torque,  $M$ , is also represented within this equation. It is important to note that the torques generated by the four rotors provide the primary source of torque for the quadrotor.

In accordance with the parameters that rely on the density of air, the radius of the propeller, the number of blades, and the blade's geometry, lift and drag coefficients [24], the thrust generated by rotor  $i$  can be represented as  $F_i = b\Omega_i^2$ , whereas the reactive torque caused by the rotor drag is expressed as  $M_i = -k\Omega_i^2$ , where both  $k$  and  $b$  are positive parameters. It is worth noting that the drag is generated by rotor  $i$  in free air.

In the context of the four rotors, the rolling torque is determined by  $M_\phi = l(-F_2 + F_4)$ , and the pitching torque is determined by  $M_\theta = l(F_1 - F_3)$ . Additionally, the yawing torque generated by the four rotors can be expressed as  $M_\psi = C(F_1 - F_2 + F_3 - F_4)$ , where  $C$  represents the proportional coefficient. Moreover, the gyroscopic torque produced by the motor rotor and the propeller can be expressed as  $M_g = \Sigma\Omega \times H_i$ . The rotational momentum moment, denoted by  $H_i$ , is only observable in the z-axis, owing to the angular velocity generated by the motor's rotation. The rotational momentum moment  $H_i$  can be expressed as  $H_i = [0, 0, J_r \Omega_i]'$ , where  $J_r$  refers to the inertia of the z-axis. Based on the preceding equations, the complete torque can be determined using the following:

$$M = M_g + \begin{bmatrix} M_\phi \\ M_\theta \\ M_\psi \end{bmatrix} \tag{7}$$

The control inputs are computed as follows:

$$\begin{bmatrix} u_1 \\ u_2 \\ u_3 \\ u_4 \end{bmatrix} = \begin{bmatrix} T \\ M_\phi \\ M_\theta \\ M_\psi \end{bmatrix} = \begin{bmatrix} b & b & b & b \\ lb & 0 & -lb & 0 \\ 0 & -lb & 0 & lb \\ -k & k & -k & k \end{bmatrix} \begin{bmatrix} \Omega_1^2 \\ \Omega_2^2 \\ \Omega_3^2 \\ \Omega_4^2 \end{bmatrix} \tag{8}$$

In which  $u_1$  denotes the total body thrust along the z-axis,  $u_2$  and  $u_3$  denote the roll and pitch torques, respectively, and  $u_4$  denotes the yawing torque. By utilizing equations (7), and (8) and incorporating air drag, the second-order state-space form can be obtained as  $[\ddot{\phi}, \ddot{\theta}, \ddot{\psi}]' = [\ddot{p}, \ddot{q}, \ddot{r}]'$ .

$$\begin{cases} \ddot{\phi} = qr \frac{I_y - I_z}{I_x} + \frac{I_r}{I_x} q \Omega_r + \frac{l}{I_x} u_2 - \frac{K_4 l}{I_x} p \\ \ddot{\theta} = pr \frac{I_z - I_x}{I_y} - \frac{I_r}{I_y} p \Omega_r + \frac{l}{I_y} u_3 - \frac{K_5 l}{I_y} q \\ \ddot{\psi} = pq \frac{I_x - I_y}{I_z} + \frac{C}{I_z} u_4 - \frac{K_6}{I_z} r \end{cases} \tag{9}$$

Here,  $K_i$  represent positive drag coefficients and constant values. Additionally,  $\Omega_r$  is defined as the overall residual rotor angular velocity, which can be calculated as  $\Omega_r = -\Omega_1 + \Omega_2 - \Omega_3 + \Omega_4$ , where  $\Omega_i$  represent the angular velocities of the rotors.

### 3. Control problem formulation

This study aims to achieve asymptotic position and attitude tracking of the quadrotor by developing flight controllers based on the second-order sliding mode technique. Specifically, the controllers aim to ensure that  $P \rightarrow P_d$  and  $\Phi \rightarrow \Phi_d$ . To accomplish this, the control system, as described by Eqs. (3), (5), and (9) are partitioned into multiple subsystems. These subsystems, which include a fully actuated subsystem consisting of  $\ddot{z}$  and  $\ddot{\psi}$  and an underactuated subsystem comprised of  $\ddot{x}, \ddot{y}, \ddot{\phi}, \ddot{\theta}$ , are inspired by the sliding mode control approach [25]. For each subsystem, a switching sliding surface is constructed using a linear combination of the position and velocity tracking errors of one (or two) state variable(s). The resulting tracking errors are driven to zero by an independent controller to achieve the desired output tracking performance.

### 4. Controller design for fully actuated and underactuated subsystems

The primary focus of this section is to present the second-order sliding mode control (2-SMC) method used to design the flight controller for the quadrotor illustrated Figure 2.

The fully actuated subsystem of the quadrotor is controlled using the 2-SMC approach to ensure that the state variables  $[z, \psi]$  converge to their respective desired values  $[z_d, \psi_d]$ . Additionally, since the quadrotor is a rigid body, the symmetry condition  $I_x = I_y$  is taken into account[19].

The sliding manifolds for the fully actuated subsystem are defined as follows:

$$s_1 = c_z(z_d - z) + (\dot{z}_d - \dot{z}) \tag{10}$$

$$s_2 = c_\psi(\psi_d - \psi) + (\dot{\psi}_d - \dot{\psi}) \tag{11}$$

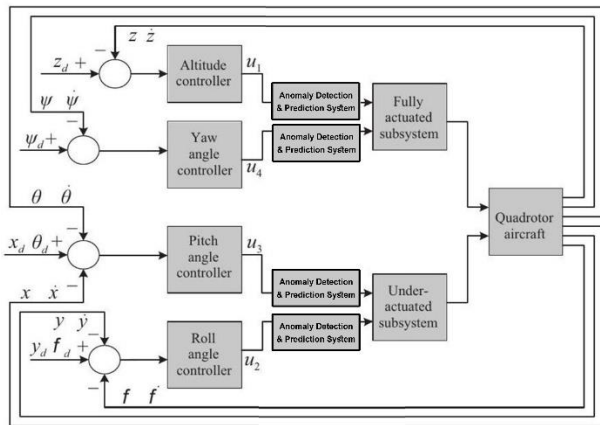


Figure 2. Flight Control Architecture

Where the coefficients  $c_z$  and  $c_\psi$  are both greater than zero. To design the corresponding control laws, the sliding surface dynamics are defined as  $\dot{s}_i = -\varepsilon_i \text{sgn}(s_i) - \eta_i s_i$  ( $i = 1, 2$ ).

$$u_1 = m_s \cdot \frac{c_z(z_d - \dot{z}) + \ddot{z}_d + g + d_1 + \varepsilon_1 \text{sgn}(s_1) + \eta_1 s_1}{\cos \phi \cos \theta} \quad (12)$$

$$u_4 = \frac{I_z}{c} [c_\psi(\dot{\psi}_d - \dot{\psi}) + \ddot{\psi}_d + d_2 + \varepsilon_2 \text{sgn}(s_2) + \eta_2 s_2] \quad (13)$$

The coefficients of the exponential approach laws, namely  $\varepsilon_1, \varepsilon_2, \eta_1$  and  $\eta_2$  are all greater than zero. In addition, the disturbance terms are defined as follows:

$$d_1 = \frac{K_3 \dot{z}}{m_s} \text{ and } d_2 = \frac{K_6 r}{I_z}$$

The underactuated subsystem of the quadrotor is controlled using 2-SMC to ensure that the state variables  $[x, \theta]$  and  $[y, \phi]$  converge to their respective desired values  $[x_d, \theta_d]$  and  $[y_d, \phi_d]$ .

The sliding manifolds are defined as given by [18]:

$$s_3 = c_1(\dot{x}_d - \dot{x}) + c_2(x_d - x) + c_3(\dot{\theta}_d - \dot{\theta}) + c_4(\theta_d - \theta) \quad (14)$$

$$s_4 = c_5(\dot{y}_d - \dot{y}) + c_6(y_d - y) + c_7(\dot{\phi}_d - \dot{\phi}) + c_8(\phi_d - \phi) \quad (15)$$

where the coefficients  $c_i$  ( $i = 1, \dots, 8$ ) will be obtained later from the Hurwitz stability analysis. The time derivatives of the two sliding manifolds are given by:

$$\dot{s}_3 = c_1(\dot{x}_d - \dot{x}) + c_2(\dot{x}_d - \dot{x}) + c_3(\ddot{\theta}_d - \ddot{\theta}) + c_4(\dot{\theta}_d - \dot{\theta}) \quad (16)$$

$$\dot{s}_4 = c_5(\dot{y}_d - \dot{y}) + c_6(\dot{y}_d - \dot{y}) + c_7(\ddot{\phi}_d - \ddot{\phi}) + c_8(\dot{\phi}_d - \dot{\phi}) \quad (17)$$

The corresponding control laws are obtained by setting  $\dot{s}_i = -\varepsilon_i \text{sgn}(s_i) - \eta_i s_i$  ( $i = 3, 4$ ), resulting in:

$$u_3 = \frac{I_y}{l} \left\{ \frac{c_1}{c_3}(\dot{x}_d - \dot{x}) + \frac{c_2}{c_3}(\dot{x}_d - \dot{x}) + \ddot{\theta}_d + \frac{c_4}{c_3}(\dot{\theta}_d - \dot{\theta}) + d_3 + \frac{1}{c_3}[\varepsilon_3 \text{sgn}(s_3) + \eta_3 s_3] \right\} \quad (18)$$

$$u_2 = \frac{I_x}{l} \left\{ \frac{c_5}{c_7}(\dot{y}_d - \dot{y}) + \frac{c_6}{c_7}(\dot{y}_d - \dot{y}) + \ddot{\phi}_d + \frac{c_8}{c_7}(\dot{\phi}_d - \dot{\phi}) + d_4 + \frac{1}{c_7}[\varepsilon_4 \text{sgn}(s_4) + \eta_4 s_4] \right\} \quad (19)$$

The exponential approach laws' coefficients, namely  $\varepsilon_3, \varepsilon_4, \eta_3$ , and  $\eta_4$ , are all greater than zero. Moreover, the disturbance terms are also present:

$$d_3 = -\frac{pr(I_y - I_x)}{I_y} + \frac{J_r p \Omega_r}{I_y} + \frac{K_5 l q}{I_y} \quad (20)$$

$$d_4 = -\frac{qr(I_y - I_z)}{I_x} - \frac{J_r q \Omega_r}{I_x} + \frac{K_4 l p}{I_x} \quad (21)$$

**Theorem:** The present study establishes the stability of the nonlinear system for the quad-rotor's dynamical model under the flight controller design presented in Eqs. (12), (13), (18), and (19). Theorem results demonstrate the effectiveness of the designed controllers in achieving system stability.

**Proof:** To demonstrate the effectiveness of the control laws  $u_i$  ( $i = 1, 2, 3, 4$ ) in achieving sliding mode control, we consider the Lyapunov function candidates:

$$V_i = \frac{1}{2} s_i^2 \quad (i = 1, 2, 3, 4) \quad (22)$$

Using Eqs. (10) and (12), (11) and (13), (16) and (17), (19b) and (20b), we obtain the time derivatives of  $V_i$ :

$$\dot{V}_i = s_i \cdot \dot{s}_i = -\varepsilon_i |s_i| - \eta_i s_i^2 \leq 0 \quad (23)$$

Therefore, all the system state trajectories can reach and remain on the corresponding sliding surfaces as desired [20].

To avoid repetition of the same steps, we illustrate the solving process for the coefficients  $c_i$  ( $i = 1, 2, 3, 4$ ) by considering the example of  $s_3$  and  $s_4$  sliding manifolds, which are obtained using the same condition on Hurwitz stability.

Firstly, we set  $\dot{s}_3 = 0$  and replace  $u_3$  with  $\theta$  in Eq. (19a), resulting in:

$$\dot{\theta}_d - \dot{\theta} = -\frac{c_1}{c_3}(\dot{x}_d - \dot{x}) - \frac{c_2}{c_3}(\dot{x}_d - \dot{x}) - \frac{c_4}{c_3}(\dot{\theta}_d - \dot{\theta}) \quad (24)$$

If  $s_3 = 0$ :

$$\begin{aligned} \dot{x}_d - \dot{x} &= -\frac{c_2}{c_1}(\dot{x}_d - \dot{x}) - \frac{c_3}{c_1}(\dot{\theta}_d - \dot{\theta}) - \frac{c_4}{c_1}(\dot{\theta}_d - \dot{\theta}), \\ \dot{\theta}_d - \dot{\theta} &= -\frac{c_1}{c_3}(\dot{x}_d - \dot{x}) + \frac{c_2^2}{c_1 c_3}(\dot{x}_d - \dot{x}) + \left( \frac{c_2}{c_1} - \frac{c_4}{c_3} \right) (\dot{\theta}_d - \dot{\theta}) + \frac{c_2 c_4}{c_1 c_3}(\dot{\theta}_d - \dot{\theta}) \end{aligned} \quad (25)$$

We define the variables  $y_1 = \dot{\theta}_d - \dot{\theta}$ ,  $y_2 = \dot{\theta}_d - \dot{\theta}$ , and  $y_3 = \dot{x}_d - \dot{x}$ . By rearranging the system equations, we obtain the cascaded form:

$$\begin{aligned} \dot{y}_1 &= y_2 \\ \dot{y}_2 &= -\frac{c_1}{c_3}(\dot{x}_d - \dot{x}) + \frac{c_2^2}{c_1 c_3}(\dot{x}_d - \dot{x}) + \left( \frac{c_2}{c_1} - \frac{c_4}{c_3} \right) (\dot{\theta}_d - \dot{\theta}) + \frac{c_2 c_4}{c_1 c_3}(\dot{\theta}_d - \dot{\theta}) \\ \dot{y}_3 &= -\frac{c_2}{c_1}(\dot{x}_d - \dot{x}) - \frac{c_3}{c_1}(\dot{\theta}_d - \dot{\theta}) - \frac{c_4}{c_1}(\dot{\theta}_d - \dot{\theta}). \end{aligned} \quad (26)$$

As the state variables approach their equilibrium points, namely  $\theta \rightarrow \theta_d$ ,  $\dot{\theta} \rightarrow \dot{\theta}_d$ ,  $x \rightarrow x_d$ , and  $\dot{x} \rightarrow \dot{x}_d$ , the variables  $y_1, y_2$ , and  $y_3$  tend towards zero.

Following linearization around the equilibrium points, the cascaded form can be expressed in a new form:

$$\begin{aligned} \dot{y}_1 &= y_2, \\ \dot{y}_2 &= -\frac{c_1}{c_3} \left[ \dot{x}_d - (-y_1 \cos \phi \cos \psi + \sin \phi \sin \psi) \frac{u_1}{m_s} + d_1 \right] \\ &+ \frac{c_2^2}{c_1 c_3} (\dot{x}_d - \dot{x}) + \left( \frac{c_2}{c_1} - \frac{c_4}{c_3} \right) (\dot{\theta}_d - \dot{\theta}) + \frac{c_2 c_4}{c_1 c_3} (\dot{\theta}_d - \dot{\theta}) \\ &+ \xi_1 y_1 + \xi_2 y_2 + \xi_3 y_3 \\ \dot{y}_3 &= -\frac{c_2}{c_1} (\dot{x}_d - \dot{x}) - \frac{c_3}{c_1} (\dot{\theta}_d - \dot{\theta}) - \frac{c_4}{c_1} (\dot{\theta}_d - \dot{\theta}) \end{aligned} \quad (27)$$

We define the column vector  $Y = [y_1 \ y_2 \ y_3]^T$ , which allows us to represent the system in matrix form as

$\dot{Y} = AY + BY$ , where A and B are appropriately sized matrices.

$$A = \begin{bmatrix} 0 & 1 & 0 \\ A_{21} & A_{22} & A_{23} \\ a & b & c \end{bmatrix} \text{ and } B = \begin{bmatrix} 0 & 0 & 0 \\ \xi_1 & \xi_2 & \xi_3 \\ 0 & 0 & 0 \end{bmatrix} \quad (28)$$

The parameters  $\xi_i (i = 1,2,3)$  are assumed to be small and constant. The term  $\lambda_{\text{left}}(A)$  denotes the real part of the leftmost eigenvalue of matrix A in the negative half-plane. When  $\lambda_{\text{left}}(A) \ll 0$ , or in other words, when A is Hurwitz, the system is asymptotically stable in the vicinity of the equilibrium points [18]. As a result, it is only necessary to investigate the stability of  $\dot{Y} = AY$ .

If we assume  $c_1 \neq 0, c_3 \neq 0$ , we can obtain the parameters:

$$A_{21} = -\frac{c_1 u_1}{c_3 m_s} \cos \phi \cos \psi + \frac{c_2 c_4}{c_1 c_3}, A_{22} = \frac{c_2}{c_1} - \frac{c_4}{c_3},$$

$$A_{23} = \frac{c_2^2}{c_1 c_3}, a = -\frac{c_4}{c_1}, b = -\frac{c_3}{c_1}, c = -\frac{c_2}{c_1}$$

$$\text{Let } |\lambda I - A| = 0, \text{ i.e., } \begin{vmatrix} \lambda & -1 & 0 \\ -A_{21} & \lambda - A_{22} & -A_{23} \\ -a & -b & \lambda - c \end{vmatrix} = 0 \quad (29)$$

The equation is expressed as

$$\lambda^3 - (A_{22} + c)\lambda^2 + (cA_{22} - A_{21} - bA_{23})\lambda + cA_{21} - aA_{23} = 0 \quad (30)$$

By letting the characteristic equation be  $(\lambda + 1)(\lambda + 2)(\lambda + 3) = 0$  and comparing the resulting coefficients with the original equation, we can obtain the values of the coefficients  $c_i (i = 1, 2,3,4)$ .

$$\begin{cases} \frac{c_4}{c_3} = 6 \\ \frac{c_1 u_1}{c_3 m_s} \cos \phi \cos \psi = 11. \\ \frac{c_2 u_1}{c_3 m_s} \cos \phi \cos \psi = 6 \end{cases} \quad (31)$$

To obtain the coefficients of the sliding manifolds, we assume that  $c_3 = 1$  and solve for the remaining coefficients using a similar approach. Specifically, we first set up the characteristic equation and solve for the coefficients using the eigenvalues of the matrix A. For example, we can set  $c_1 = 11m_s/(u_1 \cos \phi \cos \psi)$ ,  $c_2 = 6m_s/(u_1 \cos \phi \cos \psi)$ , and  $c_4 = 6$ .

It is important to note that the linearization around the state equilibrium points introduces deviation terms  $\xi_i$ , which can result in uncertain deviations from the coefficient of  $u_1$  in the first equation of (5). However, we address this issue using the SMC laws' switching gain (18).

Similarly, we obtain the coefficients  $c_5, c_6, c_7$ , and  $c_8$  using the same approach with the simplified values of  $c_5 = -11m_s/(u_1 \cos \psi)$ ,  $c_6 = -6m_s/(u_1 \cos \psi)$ ,  $c_7 = 1$ , and  $c_8 = 6$ .

The initial position and angle values of our quadrotor for simulation are  $[0, 0, 0]$  m and  $[0, 0, 0]$  rad, other parameters of our tested quadrotor are listed in Table 1. Control parameters are listed in Table 2.

**Table 1.** Quadrotor Model Parameters

Variables	Values	Units
$m_s$	1.1	kg
$l$	0.21	m
$I_x = I_y$	1.22	Ns <sup>2</sup> /rad
$I_z$	2.2	Ns <sup>2</sup> /rad
$I_r$	0.2	Ns <sup>2</sup> /rad
$K_i (i = 1, 2, 3)$	0.1	Ns/m
$K_i (i = 4, 5, 6)$	0.12	Ns/m
$g$	9.81	m/s <sup>2</sup>
$b$	5	Ns <sup>2</sup>
$k$	2	N/ms <sup>2</sup>
$c$	1	

**Table 2.** Controller Parameters

Variables	Values	Variables	Values
$c_z$	1	$c_\psi$	1
$\epsilon_1$	0.8	$\epsilon_2$	0.8
$\eta_1$	2	$\eta_2$	2
$c_1$	$11m_s/(u_1 \cos \phi \cos \psi)$	$c_5$	$-11m_s/(u_1 \cos \psi)$
$c_2$	$6m_s/(u_1 \cos \phi \cos \psi)$	$c_6$	$-6m_s/(u_1 \cos \psi)$
$c_3$	1	$c_7$	1
$c_4$	6	$c_8$	6
$\epsilon_3$	0.5	$\epsilon_4$	0.5
$\eta_3$	5	$\eta_4$	5

## 5. Anomaly detection and prediction system

To enhance the safety and reliability of position and attitude tracking control of a small quadrotor UAV, In the context of Industry 4.0 and the increasing integration of digital, physical, and human aspects, reliability engineering needs to adapt it highlights the importance of machine learning methods, such as Autoencoder, in addressing reliability concerns. The paper suggests new research directions in areas [26]; we propose using the Autoencoder method for implementing anomaly detection. The Autoencoder is a type of neural network that can learn to encode and decode data, and it can be trained on normal data to detect any deviations from it. In our approach, we use the Autoencoder to identify any unexpected behaviour of the quadrotor in real time. This allows the quadrotor to take corrective actions in case of anomalies, significantly improving its safety and reliability. Our proposed approach can find applications in various domains, such as surveillance, inspection, and search and rescue [8].

We used a deep Autoencoder with multiple hidden layers to encode and decode the input data. The encoder and decoder are fully connected layers with ReLU and Softmax activation functions. We trained the Autoencoder on a large dataset of normal motion data from Angular Velocity, Euler angle and Velocity data



from simulation and used it to reconstruct the input data. We calculated the reconstruction error as the MSE between the input and reconstructed data. We set a threshold value for the reconstruction error based on the error distribution on the training data. An input data point with a reconstruction error above the threshold was considered an anomaly [28].

For testing the system, we use the Control algorithm failure approach on our system. This fault can occur due to software bugs, incorrect parameter tuning, or limitations in the control system's algorithms and models.

**Table 3.** Positions and angles reference

Variables	Values	Time (s)
$[x_d, y_d, z_d]$	[0.6,0.6,0.6]m	0
	[0.3,0.6,0.6]m	10
	[0.3,0.3,0.6]m	20
	[0.6,0.3,0.6]m	30
	[0.6,0.6,0.6]m	40
	[0.6,0.6,0.0]m	50
$[\phi_d, \theta_d, \psi_d]$	[0.0,0.0,0.5]rad	10
	[0.0,0.0,0.0]rad	60

From simulations, Fig. 3 illustrates the trajectory of the quadrotor, which follows a set-point position and angle control. Table 3 lists reference positions and angles during the quadrotor's flight at various intervals.

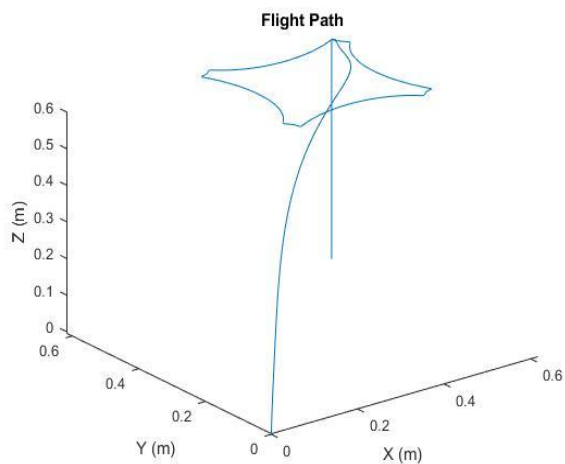


**Figure 3.** Quadrotor's path in set point position and angle control

After 60 seconds of tracking desired trajectories system adapts and learns from data produced by the control subsystem, and the system can identify the anomalies.

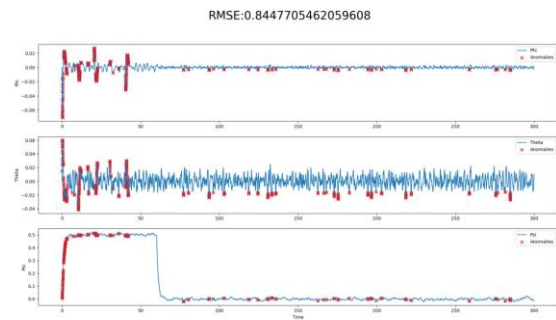


**Figure 4.** Euler angle

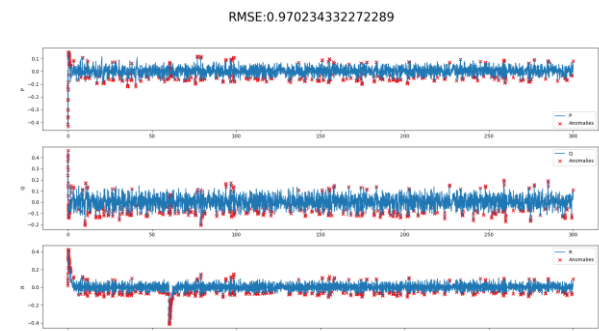


**Figure 5.** Angular Velocity

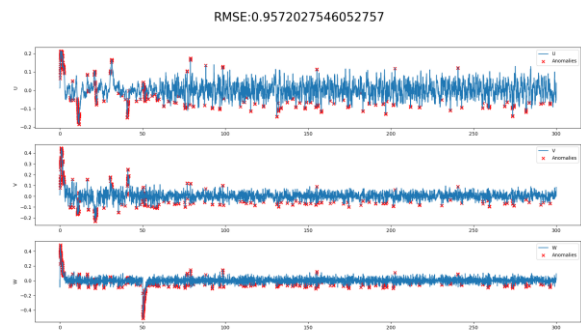


**Figure 6.** Velocity

We evaluated our method's performance on a real-world flight data dataset. We split the dataset into training and testing sets and trained the Autoencoder on the training data. We tested the method's performance on the testing data by comparing the reconstruction error of each data point with the threshold value. Our results show that the Autoencoder model could detect anomalies in the flight data with an overall MSE of 0.95 for velocity, 0.98 for angular velocity, and 0.84 for Euler angles. The high accuracy of the method demonstrates its potential for detecting anomalies in-flight data.

Our results show that the Autoencoder model is an effective approach for anomaly detection in-flight data. The high accuracy of the method indicates that it can be used to identify anomalies in various aspects of flight data. The approach can be applied to various aviation applications, such as aircraft maintenance, safety monitoring, and incident investigation. One limitation of our method is that it requires a large amount of training

data to achieve high accuracy. Future work can explore ways to reduce the required training data or improve the method's performance with smaller datasets.

In this paper also, we propose an effective approach for enhancing the safety and reliability of position and attitude tracking control of a small quadrotor UAV by using the VAR method to predict true future values. The VAR model is a statistical model that can forecast future values of a time series based on its past values. In our approach, we use the VAR method to predict the future values of the quadrotor's position and attitude, enabling it to take corrective actions in advance if necessary. Our proposed approach can significantly improve the safety and reliability of the quadrotor UAV, making it suitable for various applications, such as surveillance, inspection, and search and rescue [27].

The VAR model is a system of  $p$  linear equations that express each variable  $y_t$  as a linear combination of its past values and the past values of other variables in the system. The VAR( $p$ ) model can be written as follows: [25]

$$y_t = c + \Phi_1 y(t-1) + \Phi_2 y(t-2) + \dots + \Phi_p * y(t-p) + \epsilon_t \quad (32)$$

Where  $y_t$  is a  $p \times 1$  vector of variables at time  $t$ ,  $c$  is a  $p \times 1$  vector of intercepts,  $\Phi_i$  is  $p \times p$  matrices of coefficients for the  $i$ -th lag of the variables, and  $\epsilon_t$  is a  $p \times 1$  vector of error terms that are assumed to be independently and identically distributed with mean zero and covariance matrix  $\Sigma$ .

The VAR model can be estimated using ordinary least squares (OLS) or maximum likelihood estimation (MLE), and the predicted values can be obtained by recursively using the estimated coefficients and past values of the variables. The forecasted values for the horizon  $h$  can be obtained by multiplying the lagged values of the variables with the estimated coefficients and summing them up. The formula for the forecasted values for horizon  $h$  is:

$$y(t+h|t) = c + \Phi_1 y(t+h-1|t) + \Phi_2 y(t+h-2|t) + \dots + \Phi_p * y(t+h-p|t) \quad (33)$$

where  $y(t+h|t)$  is the forecasted value of the variable  $y$  for horizon  $h$ , based on the information available up to time  $t$ .

In this article, we use the VAR method to predict the velocity, angular velocity, and Euler angles of a small quadrotor UAV to enhance the safety and reliability of its position and attitude tracking control. We use the VAR model to forecast future values of the time series data based on its past values. The predicted values are then compared with the actual values using the mean squared error (MSE) metric to evaluate the performance of the proposed method.

Our simulation results demonstrate that the proposed VAR-based prediction method can effectively predict the velocity, angular velocity, and Euler angles of the quadrotor UAV. The MSE values obtained for the predicted values were low, indicating the high accuracy of the prediction method. Moreover, the predicted values

closely matched the actual values, confirming the effectiveness of the proposed method in enhancing the safety and reliability of the quadrotor UAV's position and attitude-tracking control.

As we can see, the result for prediction in the next hour of each sensor data can be like below:

RMSE:0.0017

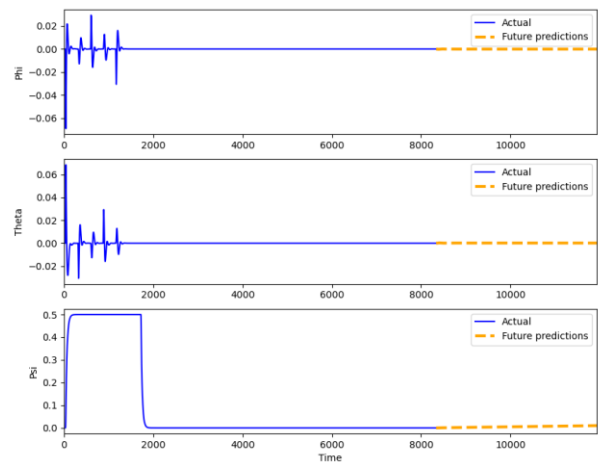


Figure 7. Euler angle prediction

RMSE:0.0022

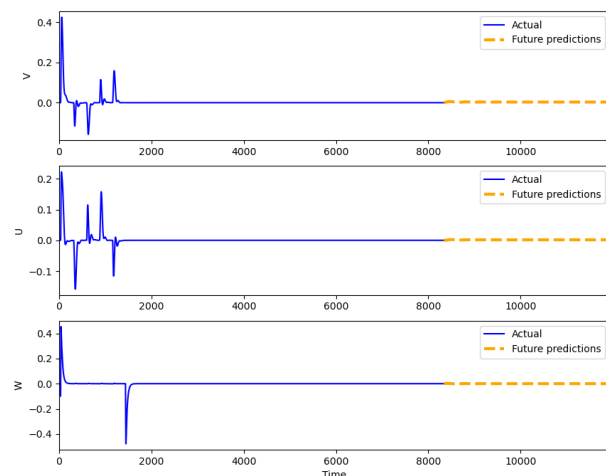


Figure 8. Velocity prediction

The performance of the proposed VAR-based prediction method is evaluated using the mean squared error (MSE) metric, which measures the difference between the predicted and actual values. The results show that the VAR model could accurately predict future values of the flight data with an overall MSE of 0.0021 for velocity, 0.00022 for angular velocity, and 0.0016 for Euler angles. These low MSE values indicate that the VAR model effectively predicted the flight data's future values. Our simulation results demonstrate that the proposed VAR-based prediction method effectively accurately predicts the velocity, angular velocity, and Euler angles of the quadrotor UAV. The MSE values



obtained for the predicted values were low, indicating a near-zero error. This result confirms the effectiveness of the proposed method in enhancing the safety and reliability of the quadrotor UAV's position and attitude-tracking control. The low and near zero MSE values obtained for the VAR prediction are promising results, indicating that the proposed method can potentially improve the performance of small quadrotor UAVs in various applications, such as surveillance, inspection, and search and rescue.

The combination of the Autoencoder anomaly detection system and the VAR prediction model has shown promising results in detecting anomalies and predicting the future values of the quadrotor's position and attitude. However, to further test the overall system's effectiveness, future plans include conducting real-world experiments with a small quadrotor UAV equipped with the developed system. The experiments will involve various flight scenarios with different levels of disturbances and external factors, such as wind and obstacles, to evaluate the system's robustness and reliability. Additionally, performance metrics, such as accuracy, sensitivity, and specificity, will be used to evaluate the system's effectiveness further. Overall, the plan is to demonstrate the practicality and usefulness of the developed system for enhancing the safety and reliability of small quadrotor UAVs.

RMSE:0.0002

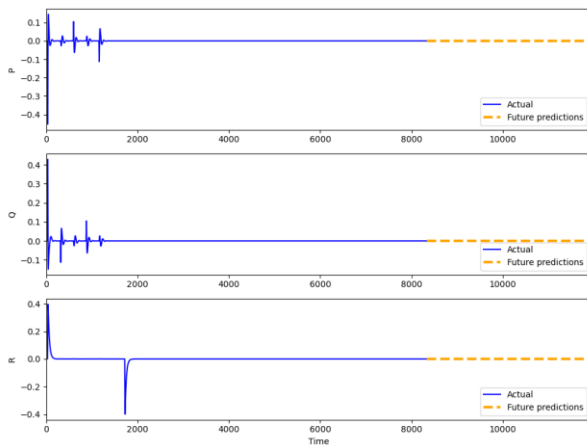


Figure 9. Angular velocity prediction

## 6. Conclusion

In summary, this paper has presented several key conclusions. Firstly, the system's state variables converge to their respective reference values, even when these values are abruptly changed at different times. Secondly, adjusting reference positions can vary the quadrotor's path, while different reference angles lead to varied attitudes. Thirdly, the system's position and velocity tracking errors approach zero, indicating convergence of the sliding variables to their sliding surfaces. Lastly, the designed controller is robust, and the proposed control

scheme has been proven effective. Overall, the simulation results presented in this paper are highly promising.

In addition to the above conclusions, the paper demonstrates the effectiveness of using an Autoencoder model for anomaly detection in-flight data, achieving low MSE results of velocity, angular velocity, and Euler angles data. Moreover, the paper presents a novel approach for predicting anomalies using a VAR model, which further enhances the safety and reliability of the quadrotor. The high accuracy and robustness of the proposed control scheme, coupled with the advanced anomaly detection and prediction capabilities, make it a highly promising approach for designing safe and reliable controllers for quadrotor UAVs. The results of this paper open up new avenues for applying advanced machine learning and control techniques in autonomous systems.

## 7. References

- [1] N. Elmeseiry, N. Alshaer, and T. Ismail, "A detailed survey and future directions of unmanned aerial vehicles (uavs) with potential applications," *Aerospace*, vol. 8, no. 12, p. 363, 2021.
- [2] Z. Ameli, Y. Aremanda, W. A. Friess, and E. N. Landis, "Impact of UAV hardware options on bridge inspection mission capabilities," *Drones*, vol. 6, no. 3, p. 64, 2022.
- [3] B. Chen, "Research on AI application in the field of quadcopter UAVs," in *2020 IEEE 2nd International Conference on Civil Aviation Safety and Information Technology (ICCASIT, 2020: IEEE*, pp. 569-571.
- [4] J. Senthilnath, M. Kandukuri, A. Dokania, and K. Ramesh, "Application of UAV imaging platform for vegetation analysis based on spectral-spatial methods," *Computers and Electronics in Agriculture*, vol. 140, pp. 8-24, 2017.
- [5] D. A. Gandhi and M. Ghosal, "Novel low cost quadcopter for surveillance application," in *2018 International Conference on Inventive Research in Computing Applications (ICIRCA), 2018: IEEE*, pp. 412-414.
- [6] M. Bajelani, M. Tayefi, and M. Zhu, "A real-test and simulation combined platform for developing intelligent tracking control of multirotors," *International Journal of Intelligent Unmanned Systems*, no. ahead-of-print, 2022.
- [7] M. Eghlimi, M. Azimi, and A. Alikhani, "Fault-tolerant Sliding Mode Controller and Active Vibration Control Design for Attitude Stabilization of a Flexible Spacecraft in the Presence of Bounded Disturbances," *International Journal of Reliability, Risk and Safety: Theory and Application*, vol. 5, no. 1, pp. 85-91, 2022.
- [8] B. Wang, Z. Wang, L. Liu, D. Liu, and X. Peng, "Data-driven anomaly detection for UAV sensor data based on deep learning prediction model," in

- 2019 Prognostics and System Health Management Conference (PHM-Paris), 2019: IEEE, pp. 286-290.
- [9] M. Bouchoucha, S. Seghour, and M. Tadjine, "Classical and second order sliding mode control solution to an attitude stabilization of a four rotors helicopter: From theory to experiment," in 2011 IEEE International Conference on Mechatronics, 2011: IEEE, pp. 162-169.
- [10] S. U. Din, Q. Khan, F.-U. Rehman, and R. Akmeliawanti, "A comparative experimental study of robust sliding mode control strategies for underactuated systems," *IEEE Access*, vol. 5, pp. 10068-10080, 2017.
- [11] H. Ríos, R. Falcón, O. A. González, and A. Dzul, "Continuous sliding-mode control strategies for quadrotor robust tracking: Real-time application," *IEEE Transactions on Industrial Electronics*, vol. 66, no. 2, pp. 1264-1272, 2018.
- [12] M. Herrera, W. Chamorro, A. P. Gómez, and O. Camacho, "Sliding mode control: An approach to control a quadrotor," in 2015 Asia-Pacific Conference on Computer Aided System Engineering, 2015: IEEE, pp. 314-319.
- [13] F. Sharifi, M. Mirzaei, B. W. Gordon, and Y. Zhang, "Fault tolerant control of a quadrotor UAV using sliding mode control," in 2010 conference on control and Fault-Tolerant Systems (SysTol), 2010: IEEE, pp. 239-244.
- [14] A. Benallegue, A. Mokhtari, and L. Fridman, "High-order sliding-mode observer for a quadrotor UAV," *International Journal of Robust and Nonlinear Control: IFAC-Affiliated Journal*, vol. 18, no. 4-5, pp. 427-440, 2008.
- [15] C. Coza, C. Nicol, C. Macnab, and A. Ramirez-Serrano, "Adaptive fuzzy control for a quadrotor helicopter robust to wind buffeting," *Journal of Intelligent & Fuzzy Systems*, vol. 22, no. 5-6, pp. 267-283, 2011.
- [16] I. Eker, "Second-order sliding mode control with experimental application," *ISA transactions*, vol. 49, no. 3, pp. 394-405, 2010.
- [17] S. Mondal and C. Mahanta, "A fast converging robust controller using adaptive second order sliding mode," *ISA transactions*, vol. 51, no. 6, pp. 713-721, 2012.
- [18] Z.-Q. Guo, J.-X. Xu, and T. H. Lee, "Design and implementation of a new sliding mode controller on an underactuated wheeled inverted pendulum," *Journal of the Franklin Institute*, vol. 351, no. 4, pp. 2261-2282, 2014.
- [19] H. Ashrafiuon and R. S. Erwin, "Sliding mode control of underactuated multibody systems and its application to shape change control," *International Journal of Control*, vol. 81, no. 12, pp. 1849-1858, 2008.
- [20] E.-H. Zheng, J.-J. Xiong, and J.-L. Luo, "Second order sliding mode control for a quadrotor UAV," *ISA transactions*, vol. 53, no. 4, pp. 1350-1356, 2014.
- [21] R. Olfati-Saber, "Nonlinear control of underactuated mechanical systems with application to robotics and aerospace vehicles," Massachusetts Institute of Technology, 2001.
- [22] G. V. Raffo, M. G. Ortega, and F. R. Rubio, "An integral predictive/nonlinear  $H_\infty$  control structure for a quadrotor helicopter," *Automatica*, vol. 46, no. 1, pp. 29-39, 2010.
- [23] G. V. Raffo, M. G. Ortega, and F. R. Rubio, "Backstepping/nonlinear  $H_\infty$  control for path tracking of a quadrotor unmanned aerial vehicle," in 2008 American Control Conference, 2008: IEEE, pp. 3356-3361.
- [24] R. W. Prouty, *Helicopter performance, stability, and control*. 1995.
- [25] Z. Weidong, Z. Pengxiang, W. Changlong, and C. Min, "Position and attitude tracking control for a quadrotor UAV based on terminal sliding mode control," in 2015 34th Chinese control conference (CCC), 2015: IEEE, pp. 3398-3404.
- [26] M. A. Farsi and E. Zio, "Industry 4.0: Some challenges and opportunities for Reliability Engineering," *International Journal of Reliability, Risk and Safety: Theory and Application*, vol. 2, no. 1, pp. 23-34, 2019.
- [27] D. Bank, N. Koenigstein, and R. Giryes, "Autoencoders," *arXiv preprint arXiv:2003.05991*, 2020.
- [28] N. Kilbertus, M. J. Kusner, and R. Silva, "A class of algorithms for general instrumental variable models," *Advances in Neural Information Processing Systems*, vol. 33, pp. 20108-20119, 2020.